International Journal of Energy
ISSN: 2957-9473 | Vol. 2, No. 3, 2023

Analysis of the Migration of Carbon Dioxide in Deep Saline Fractured Aquifer

Bin Liu [1,*], Chen Xu [1], Junchang Sun [2], Hongqi Yuan [3]

[1] School of Electrical Engineering & Information, Northeast Petroleum University, Heilongjiang, China
[2] Bohai Rim Energy Research Institute, Northeast Petroleum University, Hebei, China
[3] School of Earth Sciences, Northeast Petroleum University, Heilongjiang, China

*** Corresponding author:** Bin Liu (Email: liubin.nepu@hotmail.com)

Abstract: In order to control greenhouse gases and protect the environment, carbon dioxide emission reduction has become a global research hotspot. Fractures in the deep saline aquifer enhance the heterogeneity of the aquifer, and have an important effect on CO_2 migration, thus the detailed description and characterization of fractures in geological structure are very important. Existing research on the impact of fractures on CO_2 migration, however, ignores the role that the fractures' characteristics play in this process. This work aims at addressing this gap. Based on the embedded discrete fractured model (EDFM), we quantified the role of the fractures in the mechanism of CO_2 migration and studied the length, aperture, and orientation of the fractures. It is found that the CO_2 plume takes the fracture as its preferred channel and changes the migration direction. The longer the fracture length and wider the fracture aperture, the faster the CO_2 migration rate is. The change in fracture orientation mainly affects the migration direction of the CO_2 plume. Due to the different angles of the plume entering the fracture, the influences on the CO_2 migration rate are also different. When the orientation is 45°, the CO_2 migration rate is the fastest, while it is the slowest at 135°. When there is a complex fracture network in the aquifer, the heterogeneity of the aquifer is enhanced. Compared with the non-fractured aquifer, the direction and rate of CO_2 migration are greatly changed, and the instability of CO_2 sequestration is increased.

Keywords: Deep Saline Fractured Aquifer; Migration of Carbon Dioxide; EDFM.

1. Introduction

Carbon dioxide geological sequestration is one of the major technologies to significantly reduce anthropogenic greenhouse gas emissions [1]. Because of their potential for huge storage capacities and widespread dispersion worldwide, deep saline aquifers are attractive storage sites. Due to the existence of geological heterogeneity, fractures, and faults, fluid migration in the process of CO_2 sequestration is complicated.

Many researchers have worked on CO_2 sequestration in fractured reservoirs. To model CO_2 evolution in fractured saline aquifers, Ren *et al.*[2] suggested a two-phase flow unified pipe network technique. Iding *et al.*[3] constructed an analytical solution of one-dimensional flow of CO_2 in fractures and dissolution into the matrix. On the basis of a fully implicit cell-centered finite volume approach on unstructured grids, Ahmed *et al.* [4]provided a simulation of compressible two-phase flow of components in fractured porous media. Du *et al.*[5] built the 3D embedded discrete fractured model (EDFM) to simulate the inter-fracture CO_2 flooding and geological storage process in fractured reservoirs. Shafabakhsh *et al.*[6] investigated the impacts of fracture characteristics and topological structures on the domain's storage capacity at various rates of CO_2 mineral dissolution based on the numerical modeling of a hypothetical reservoir.

The idea of CO_2-saline two-phase migration and EDFM measurement of reservoir fractures serve as the foundation for this work. The impact of fracture characteristics on the migration of CO_2 in saline water was modelled using a 2D reservoir model to build a numerical modeling approach for CO_2-saline two-phase flow. A complex fracture network aquifer's CO_2-saline migration is contrasted with that of an unfractured aquifer.

2. Governing Equations and Conceptual and Numerical Models

2.1. Mathematical Model

The studies of Lee *et al.*[7], Li and Lee[8], and Moinfar *et al.*[9] are the foundation for the mathematical formulation. For a model with N_f fractures, mass-conservation equations are used to define flow in N_f fractures in a model, index i represent the fractures. For all $i \in [1, N_f]$,

$$\frac{\partial(\phi^i \rho_\alpha S_\alpha^i)}{\partial t} + \nabla \cdot (\rho_\alpha \vec{u}_\alpha^0) = \frac{\rho_\alpha}{a_i}\left[q_\alpha^i - q_\alpha^{i,0} - \sum_{j=1,j\neq i}^{N_f} q_\alpha^{i,j}\right], \alpha = \mathrm{l,g}. \quad (1)$$

Matrix's flow is simulated by mass conservation equation as well. Index i=0 is used to conveniently represent the matrix. For i=0,

$$\frac{\partial(\phi^0 \rho_\alpha S_\alpha^0)}{\partial t} + \nabla \cdot (\rho_\alpha \vec{u}_\alpha^0) = \rho_\alpha\left[q_\alpha^0 - \sum_{i=1}^{N_f} q_\alpha^{0,i}\right], \alpha = \mathrm{l,g}. \quad (2)$$

where, ϕ^i is the porosity of fracture i. ϕ^0 is the porosity of the matrix. ρ_α is the density of fluid phase α. a_i is the aperture of fracture i. S_α^i is the saturation of fluid phase α in fracture i. $q_\alpha^{i,0}$ is the transfer function that determines the fluid flow from fracture i to matrix, and $q_\alpha^{0,i}$ determines the opposite direction. $q_\alpha^{i,j}$ is the transfer function that determines the fluid flow from fracture i to fracture j. q_α^0 is the source/sink terms in the matrix and q_α^i is in the fractures, respectively.

Fracture equations are coupled to the matrix equations through $q_\alpha^{i,0}$ and the fracture equations are coupled with each other through $q_\alpha^{i,j}$, $q_\alpha^{i,j} = 0$ for some fracture pairs which are not intersect with each other, $\vec{u}_\alpha^i$ is the velocity of fluid phase α in medium i which is modeled by Darcy's law.

For conductive fractures, the permeability can be determined by the aperture of the fracture.

$$k_f = \frac{a^2}{12 f_c} \tag{3}$$

where, k_f is fracture permeability, a is the aperture of fracture. The correction factor f_c equals to 1 for laminar flow between parallel.

The flow of the fluid phases between the matrix-fracture cell pairs are modeled by TPFA as follows:

$$Q_\alpha^{m,f} = \int_{V_m} q_\alpha^{m,f} \, \mathrm{d}V = T^{mf} \frac{k_{r\alpha}}{\mu_\alpha} (p_\alpha^m - p_\alpha^f) \tag{4}$$

$$Q_\alpha^{f,m} = \int_{A_f} q_\alpha^{f,m} \, \mathrm{d}A = T^{mf} \frac{k_{r\alpha}}{\mu_\alpha} (p_\alpha^f - p_\alpha^m) \tag{5}$$

where, $Q_\alpha^{m,f}$ is the volumetric flow rate from the matrix cell to the fracture cell, $Q_\alpha^{f,m}$ is the opposite, and $Q_\alpha^{m,f} = -Q_\alpha^{f,m}$. V_m is the matrix cell domains and A_f is the fracture cell domains. $k_{r\alpha}/\mu_\alpha$ is the mobility term. T^{mf} is the transmissibility between each pair matrix-fracture cell.

The flow of fluid phase between the intersected fracture cell pairs, the fluid exchange is as follows:

$$Q_\alpha^{f_1,f_2} = \int_{A_{f_1}} q_\alpha^{f_1,f_2} \, \mathrm{d}A = T^{ff} \frac{k_{r\alpha}}{\mu_\alpha} (p_\alpha^{f_1} - p_\alpha^{f_2}) \tag{6}$$

$$Q_\alpha^{f_2,f_1} = \int_{A_{f_2}} q_\alpha^{f_2,f_1} \, \mathrm{d}A = T^{ff} \frac{k_{r\alpha}}{\mu_\alpha} (p_\alpha^{f_2} - p_\alpha^{f_1}) \tag{7}$$

where, the transmissibility $T^{ff} = 0$ for some fracture pairs which are not intersect with each other and positive otherwise.

2.2. Conceptual and Numerical Models

As shown in Figure 1 is a saline water saturated rectangular aquifer, the initial pressure is 10.5MPa, and the temperature is 25℃. CO_2 is injected at the bottom left corner cell at the rate of 6.5×10^{-5}PV/day[10] and the cell at the diagonally opposite corner is the observation point with the pressure of 10.5MPa. The model parameters are shown in Table 1[11].

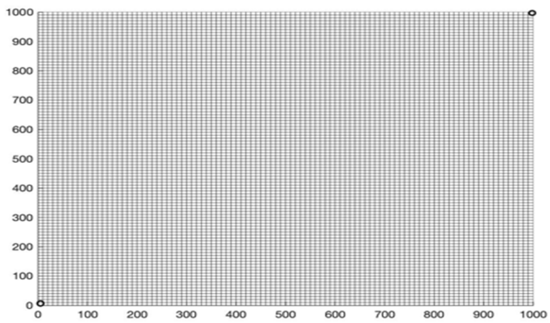

Figure 1. Concept diagram of non-fracture reservoir

Table 1. Model Parameters

Parameter	Value	Unit
Density of CO_2	714	$kg.m^{-3}$
Viscosity of CO_2	0.0577	mPa·s
Density of saline water	1121	$kg.m^{-3}$
Viscosity of saline water	1.1875	mPa·s
Matrix permeability	20	mD
Matrix porosity	0.15	—

3. Results and Discussion

In this chapter, EDFM is used to reveal the fracture, and the fractures are treated as line segments with a certain aperture in a two-dimensional matrix. The influences of the length, aperture, and orientation of the fractures on CO_2 migration are simulated. The migration difference of CO_2 in a non-fractured aquifer and a complex fractured aquifer is compared.

3.1. Different Length of Fracture

In this section, the influence of fracture length on CO_2 migration is studied. Two groups of fractures with different lengths are set, namely fracture1 and fracture2. The azimuths are 45°, and the apertures are 1mm. The migration simulation time is 10 years.

As shown in Figure 2, fractures become the preferred channel, and the migration location will fluctuate depending on the geometry of the fractures. It can be seen in Figure 2 (a) that CO_2 saturation is high and accumulates obviously at the fracture outlet, while the longer the fracture, the less the accumulation, which is because the matrix permeability is smaller than the fracture permeability. When the plume flows out of the fracture, the migration rate in the matrix slows down and the plume accumulates in the matrix, while the longer the fracture, the more the high-permeability channels in the reservoir increase.

3.2. Different Aperture of Fracture

In this section, the influence of fracture aperture on CO_2 migration is studied. Two fractures with different apertures are set as a=0.1mm and a=1mm, and the azimuths are 45°.

Figure 3 shows the migration of CO_2 with two kinds of fracture apertures. As shown in Figure 3(a), the plume does not move quickly along the fracture, and the plume front only had a short tip along the fracture because of the narrow fracture aperture and poor permeability. Figure 3 (b) shows that the plume migrates quickly along the fracture. When a=1mm, more CO_2 accumulates at the fracture outlet, which is due to the large fracture aperture, high permeability, and fast migration rate. With the further CO_2 injection, a large number of CO_2 plumes migrate within the matrix and are widely distributed in the aquifer due to the poor CO_2 migration ability of the fractures with a narrow aperture, while the fractures with a wider aperture migrate more CO_2 and have a small CO_2 distribution range in the matrix.

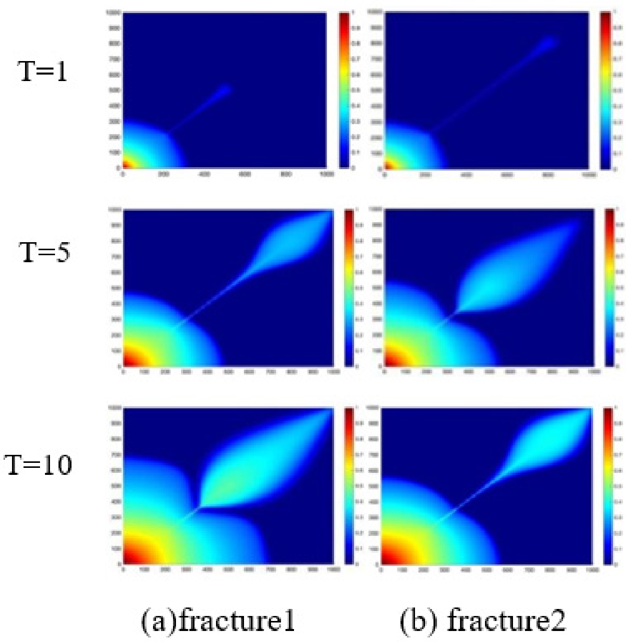

Figure 2. CO_2 gas saturation with different length

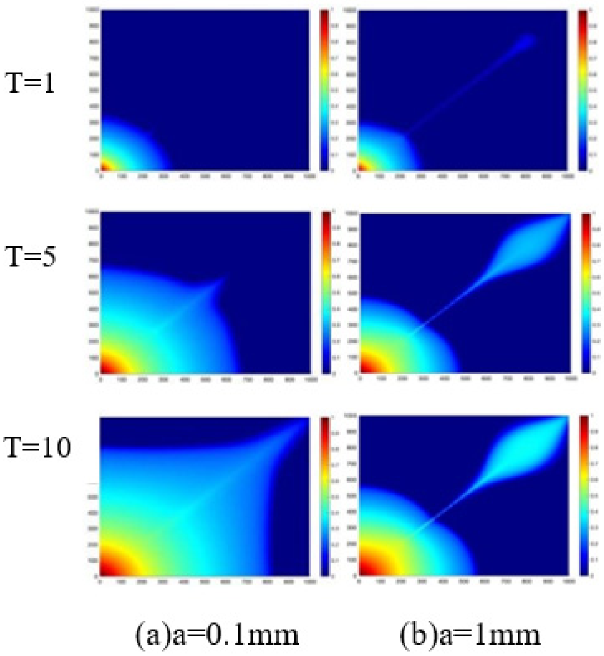

Figure 3. CO_2 gas saturation with different aperture

3.3. Different Orientation of Fracture

In this section, the influence of fracture orientation on CO_2 migration is studied. Four fractures are set with the orientations of 0°, 45°, 90°, 135°, and the length of $600\sqrt{2}$, and the apertures are 1mm, respectively.

Figure 4 shows the migration of CO_2 with four kinds of fracture orientations. It is found that the plume migrates into the fracture first when the azimuth is 45°. After 2 years of injection, the CO_2 plume arrives at the fracture with azimuths of 0° and 90° and migrates into the fracture. After 4 years and 304 days of injection, the CO_2 plume arrives at the fracture with an azimuth of 135°, and the plume enters the fracture. It is observed that CO_2 does not migrate along the fracture to both ends of the fracture, but only a small amount of CO_2 accumulates at both ends of the fracture. The direction of the CO_2 plume approaches the observation point. The reason for this phenomenon is that both ends of the fracture are on the same pressure contour line, and the pressure gradient in the advancing direction of the plume is larger than the pressure gradient generated at both ends of the fracture. The plume migrates along the direction of the larger pressure gradient. Therefore, when the fracture is perpendicular to the direction of the CO_2 plume, the fracture has little influence on the direction of CO_2 migration.

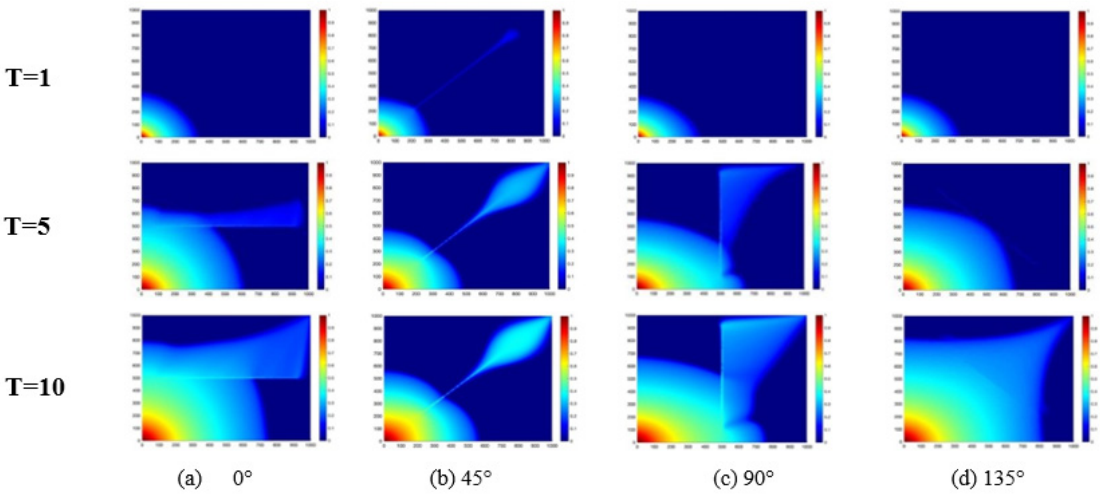

Figure 4. CO_2 gas saturation with different orientation

3.4. Complex Fracture Network

In this section, CO_2 migration with a complex fracture network is studied. A complex fracture network model is set up to compare with the non-fracture reservoir and observe its influence on CO_2 migration. The location, orientation, and length of fractures are random, and the aperture is 1mm. The model diagram is shown in Figure 5.

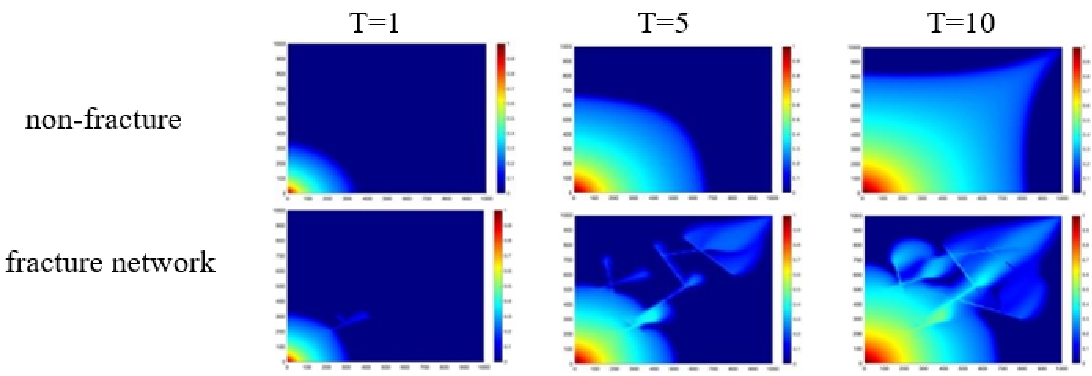

Figure 5. CO_2 gas saturation in non-fracture and complex fractured reservoirs

Figure 5 shows the migration of CO_2 in non-fractured and complex fracture reservoirs. With CO_2 injection, the CO_2 plume migrates into a symmetrical arc in the non-fracture reservoir, while in the reservoir with a complex fracture network, the CO_2 plume migrates to the fracture, changes its migration path, and accelerates its migration. After 10 years of migration, the difference in the distribution of the CO_2 plume in the reservoir can be obviously observed. CO_2 migrates preferentially through fractures in complex fractured reservoirs, so CO_2 is mainly distributed in fractures while it is evenly distributed in non-fractured reservoirs.

4. Conclusion

In this work, we investigate the role of a fracture's properties on CO_2 migration in a deep saline aquifer, including length, aperture, and orientation. We only consider the physical migration process at the initial stage of injection and ignore the dissolution and chemical processes. The embedded discrete fracture model is employed to model fractures with different lengths, apertures, and orientations. The existence of fractures has a great influence on the migration of CO_2. CO_2 migrates rapidly along the fractures and changes the original migration direction.

Results indicate that in the case of different lengths of fractures, the longer the fracture length, the higher the permeability channels, and the faster the CO_2 migration rate, which is not conducive to the physical storage of CO_2. The wider the fracture aperture, the higher the fracture permeability and the faster the CO_2 migration rate. The change in fracture orientation mainly affects the direction of CO_2 plume migration. Due to the different azimuths of plumes entering the fracture, the influences on the CO_2 migration rate are different. When the azimuth is 45°, the migration rate is the fastest, and when the azimuth is 135°, the migration rate is the slowest. The determination of the specific orientation is related to the location of the injection well, so it can also be used as a reference for the location of the injection well. The faster migration rate may lead to the rapid arrival of CO_2 at leakage points in the formation, such as faults and abandoned wells. The complexity of the fracture network has a great influence on the direction and rate of CO_2 migration in the reservoir. The existence of a complex fracture network will enhance the heterogeneity of the reservoir, form a high-permeability channel network, and accelerate CO_2 migration. Plume migrates along the high-permeability direction of fractures to accelerate the migration rate of CO_2. The specific migration should be considered in light of the properties of each fracture.

Acknowledgments

This research was funded by CNPC Innovation Found, grant number 2021DQ02-1103, National Key Research and Development Program, grant number 2022YFE0206800.

References

[1] Bachu, S., Bonijoly, D., Bradshaw, J., Burruss, R., Holloway, S., Christensen, N.P., Mathiassen, O.M., 2007. CO_2 storage capacity estimation: methodology and gaps. Int. J. Greenhouse Gas Control 1, 430–443.

[2] Feng R, Ma G , Yang W, et al. Two-phase flow pipe network method for simulation of CO_2 sequestration in fractured saline aquifers[J]. International Journal of Rock Mechanics & Mining Sciences, 2017, 98:39-53.

[3] Iding M, Blunt M J . Enhanced solubility trapping of CO_2 in fractured reservoirs[J]. Energy Procedia, 2011, 4:4961-4968.

[4] Ahmed R, Li J . A numerical framework for two-phase flow of CO_2 injection into fractured water-saturated reservoirs[J]. Advances in Water Resources, 2019, 130(AUG.):283-299.

[5] Du X, Cheng L , Liu Y , et al. Application of 3D embedded discrete fracture model for simulating CO_2 -EOR and geological storage in fractured reservoirs[J]. IOP Conference Series Earth and Environmental Science, 2020, 467:012013.

[6] Shafabakhsh P, Ataie-Ashtiani B , Simmons C T , et al. Convective-reactive transport of dissolved CO_2 in fractured-geological formations[J]. International Journal of Greenhouse Gas Control, 2021.

[7] Lee S H, Lough M F , Jensen C L . Hierarchical modeling of flow in naturally fractured formations with multiple length scales[J]. Water Resources Research, 2001, 37(3):443–455.

[8] Li L, Lee S H . Efficient Field-Scale Simulation of Black Oil in a Naturally Fractured Reservoir Through Discrete Fracture Networks and Homogenized Media[J]. SPE Reservoir Evaluation & Engineering, 2008, 11(4):750-758.

[9] Moinfar A, Varavei A , Sepehrnoori K , et al. Development of a Novel and Computationally-Efficient Discrete-Fracture Model to Study IOR Processes in Naturally Fractured Reservoirs [J]. Spe Improved Oil Recovery Symposium.

[10] Wang Y, Vuik C , Hajibeygi H . CO_2 Storage in deep saline aquifers: impacts of fractures on hydrodynamic trapping[J]. International Journal of Greenhouse Gas Control, 2022, 113:103552-.

[11] Nordbotten J M, Celia M A , Bachu S . Injection and Storage of CO_2 in Deep Saline Aquifers: Analytical Solution for CO_2 Plume Evolution During Injection[J]. Transport in Porous Media, 2005, 58(3):339-360.